SIMULATION OF THE FROST EFFECT CONSIDERING CLIMATIC CHANGE

J. PATZAK
Institute of Urban Engineering & Road Construction,
Dresden University of Technology, Germany
JOERG.PATZAK@TU-DRESDEN.DE
S. KAYSER; F. WELLNER; A. ZEISSLER
Institute of Urban Engineering & Road Construction,
Dresden University of Technology, Germany
Sascha.Kayser@tu-dresden.de; Frohmut.Wellner@tu-dresden.de;
Alexander.Zeissler@tu-dresden.de

Abstract

The global and local change of our climate system expected future needs to be considered in pavement design. The probably rising air temperature in this century leads to changed temperature conditions in pavements.
The present investigation works with this problem and analyses the effects of climate change concerning frost penetration in pavements based on numerical simulations and selected climate scenarios. Additionally forecasts of the expected changes of frost penetration in pavements will be realized. Based on these results, it will be shown which possible effects on the pavement stability may be gained by a modification of the sub base thickness.

1. INTRODUCTION

The global change of climate conditions is one of the current public topics. The reasons of the running climate change are various. It is conforming postulated, that a part of the climate changes results with high probability of human activities. For the second part of this century it was observed that the maximum and the minimum of the air temperature are increased. Thereby the increase of the daily minimum of air temperature was greater than the maximum. Additionally the number of extreme heat days increases and the number of frost days decreases. For the 21st century it is very probable that this development will go on [1]. The effects of climate change will be regionally different. The main question is which effects on existing and future pavements are possible by the projected climate changes, independent of a regional view. The basics of these investigations are numerical simulations of temperature conditions in pavements. Based on that, the first step will be to investigate the possible changes of frost in pavements, in detail frequency and depth. The following second step considers the consequence of an economical based view reducing the thickness of the frost proof layer. Under these conditions the stability of the pavement structure will be projected.

2. BASICS OF TEMPERATURE SIMULATION

The temperatures in pavements results from different processes of energy transportation (transportation by rays, conduction and convection). The environmental condition (global radiation, air temperature, humidity, wind speed, rainfall rate and cloud cover) are changing continuously and causes non steady state temperature conditions. These

problems can be solved based on thermal-physical legalities, especially by the help of energy- and thermal balance equation using an iterative calculation algorithm [13]. Next to the so called environmental condition the thermal-physical properties of pavement materials like thermal conductivity, specific heat capacity, water contend, density, reflection properties and heat transfer properties influence temperature conditions considerably.

2.1. Parameter set-ups – Definition and Identification

The thermal material properties of each pavement layer influence the temperature conditions of the whole construction and thus the frost penetration. The diversity of the used pavement materials complicates an explicit classification. For the definition of detailed material specific value extensive laboratory tests are necessary. In order to characterize the influence of single material parameters and also of the combination of different parameter settings, not single parameters but parameter ranges are determined for the numerical simulations. The used ranges result from different values of mentioned in literature [15; 18]. Based on this approach a defined range of thermal material parameters was specified. For selected climate boundary conditions the combination of the layer specific parameter set-ups shows the wanted distribution of the zero degree isothermal line and in result the depth of frost. That shows clearly influence of thermal material parameters on temperature conditions and frost penetration. Through the evaluation of different scenarios reference parameters were selected and used for the following projected calculations. Figure 1 shows the used structural selection course.

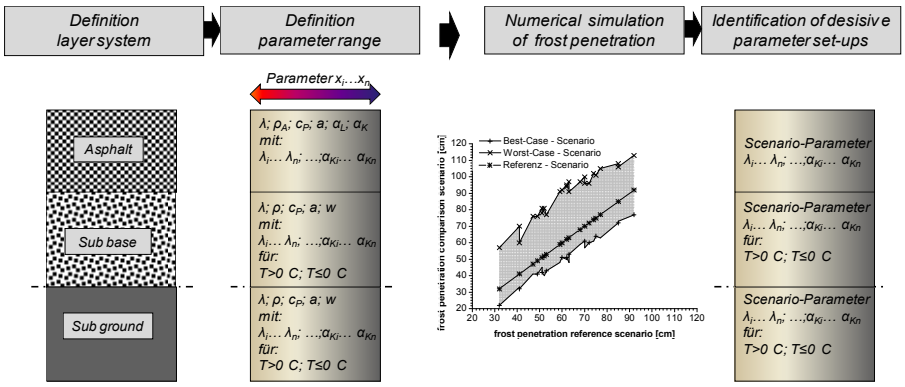

Figure 1 – Scheme: identification of thermal layer specific parameter and parameter set-ups

2.2. Detection of condition-based material parameters

It is obligatory necessary to define condition-based material parameters (that means variable parameters) in addition to the mentioned parameter boundary to get numerical calculations as exactly as possible. Following, the problem of thermal detection of unbound granular materials will be shown. It is well known, that water exists in different manifestations. Basically the term soil water describes the hole water in the sub bases of pavements. It can be divided in free moveable and bounded water inside the pore volume. Free pore water is depending on gravity and also flow forces. Hygroscopic Water (capillary water) depends on physical interaction processes and isn't free but bounded [4; 15].
Decisive for the possible part of water in the soil matrix are soil type and soil structure. Fine grained soils have a greater specific surface, partly also greater surface charges then coarse grained soils, so the water binding capacity is much greater [5]. The changes of water content and aggregate state of water in soil or unbound granular materials

concludes in changings of load bearing capacity and also in changing thermal conditions. Therefore from a thermo-physical point of view the way dividing of frozen or not frozen state of these materials is necessary. Unbound granular materials are basically 3-phases mixtures including grains, air and water. The very complex mechanisms of their interference make the detection and characterization very difficult. Thus there are often used defined states like density, particle size distribution, saturation, phase ratio or temperature for modeling. It is well known that the thermo-physical importance of the single phases is very different. Pore volume air has very poor heat conductivity. It is nearly four times smaller than the heat conductivity of water and grains. Principally the heat conductivity of soil or unbound granular materials increases with growing water content. This is caused by the 20-times greater heat conductivity of water compares to air. Also proportional is the behavior of water content and specific heat capacity. Increasing water content concludes to a higher ability to save heat energy.

There is a distinction between the complete unfrozen and complete frozen state of unbound granular materials. The thermo-physical parameters differ considerably. In completely solid state of water the heat conductivity is approximately 2,20 W/(m·K) and therefore nearly 4-times higher than in fluid state. By contrast to the heat conductivity the specific heat capacity of ice is approximately 2,12 kJ/(kg·K) and therefore only about 50 % of the specific heat capacity of water (fluid state). So the ability to transport heat energy increases during reduced heat storage and the frost penetration will be encouraged.

Water exists in nature in three aggregates (solid, fluid and gaseous). Due to heat extraction or heat input an aggregate change takes place at constant temperature. The energy level increases from the solid over the fluid to the gaseous condition. Figure 2 – shows on the left side the cooling curve of 1 kg of water during constant normal pressure. The change from gaseous to fluid phase takes place by a temperature of 100 degrees Celsius. The heat energy resulting from the condensation process is about 2256 kJ/kg. During the change from liquid to solid phase the released energy is about 334 kJ/kg (heat of crystallization). According to the law of conservation of energy the realized heat energy of crystallization is equal to the needed heat energy for melting.

The same physical correlation applies for the condensation- or evaporation process. This typically behaviour of water is invalid in combination with grains. The different kinds of bindings in grains are the cause of a variable melting point of water, that means the change of the aggregate phase takes places at different temperatures. The freezing temperature of water depends on the free enthalpy, which is reduced by decreasing binding and ion concentration [5].

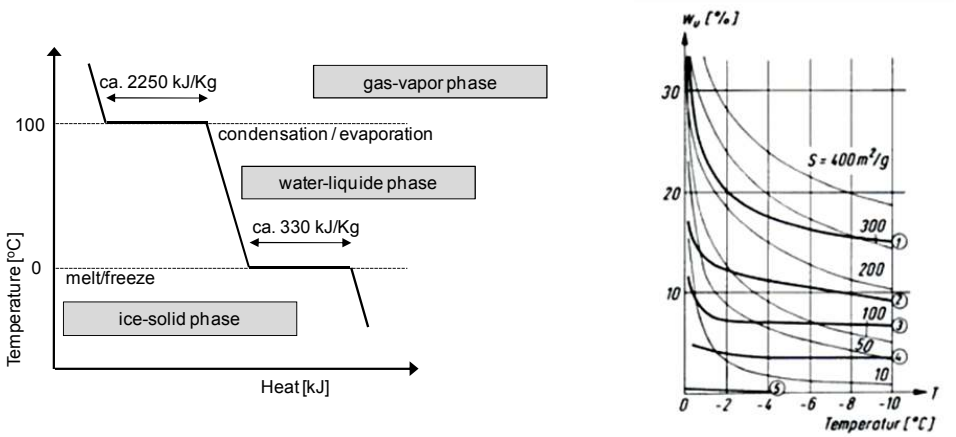

Figure 2 - Qualitative Course of the cooling curve of water (1 kg) under normal pressure depending on time t(left); unfrozen water ratio in soil for different soil types (1 clay, 2 pleistocene clay, 3 clayey low sandy silt, 4 low clayey silty sand, 5 sand) and different specific surfaces S (10 to 400 m²/g at 0°C) [Smoltczyk 2001] (right)

Water is freezing first, there where the influence of binding forces is low (great pore volume). Just with further falling temperatures, also the bound water changes its aggregate phase and becomes solid (Figure 2 – right). It is detectable that the part of unfrozen water in soils decreases with falling temperatures. In the shown curves you one see that the curve shape is different for each of the sample soil types [3]. The detailed material specific functional description can be realized only within a massive experimental effort. The description of the correlation between temperature and the unfrozen water part can be realized in a modeling way that means due to approximation of the known connections. A sample is shown on the left side of figure 3, where one can see the applied functions of description for possible soil types. The used functional classification is based on references [18; 15]. With the knowledge of the temperature depending water part depends on temperature it is possible to convert the heat energy for calculation of heat capacity (I). In the result of this process the heat capacity can be calculated depending on temperature and soil or grain (Figure 3 – right). The calculating of the thermal parameters is variable as well and depends on the water content. Only the coupling of the thermal parameters of soils and grains for the complete frozen and the complete unfrozen condition with the variable parameters while aggregate changing, delivers possibilities for adequate calculation results. Coupling describes here not a mechanical meaning of coupling (coupling of variables) but the different consideration of material specific connections during numerical simulation of heat conduction.
The results of the coupling effect are exemplary shown in figure 4. It appears that under consideration of freezing and thawing process the calculated temperatures represent the real temperatures considerably better. Therefore the temperature conditions in pavements in general and the frost penetration in particular can be calculated accurately as possible.

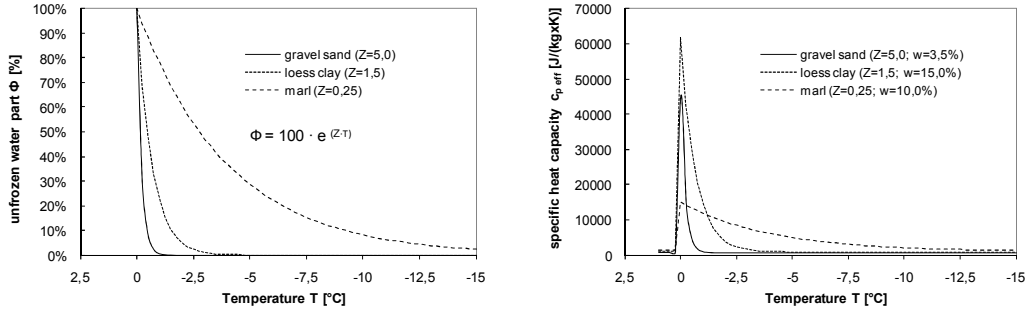

Figure 3 – Unfrozen water part depending on temperature and material (left) and the calculated specific heat capacity of the material mixture during the transition from fluid to solid state (right)

$$Cp_{\,eff} = C_W \cdot X_W + C_E \cdot X_E + \frac{1}{\Delta T} \cdot \int_{T}^{T+\Delta T} \Delta H_f \cdot \frac{\delta \Phi}{\delta T} \delta T \qquad \text{(I)}$$

with: $\frac{\delta \Phi}{\delta T} \delta T$ as alteration rate of unfrozen water over temperature interval ΔT expressed by $\Phi = f(Z;T) = e^{(Z \cdot T)}$ for $\Delta T \leq 0{,}1$ K

C_W	Heat capacity of water	[J/K]
C_E	Heat capacity of ice	[J/K]
$X_W ; X_E$	Volume parts of water and ice	[-]
ΔH_f	Melting energy per mass unit of unfrozen water	[J/K]
$\delta \Phi$	Alternation of the unfrozen water part	[-]
ΔT	Temperature alternation interval	[°C]

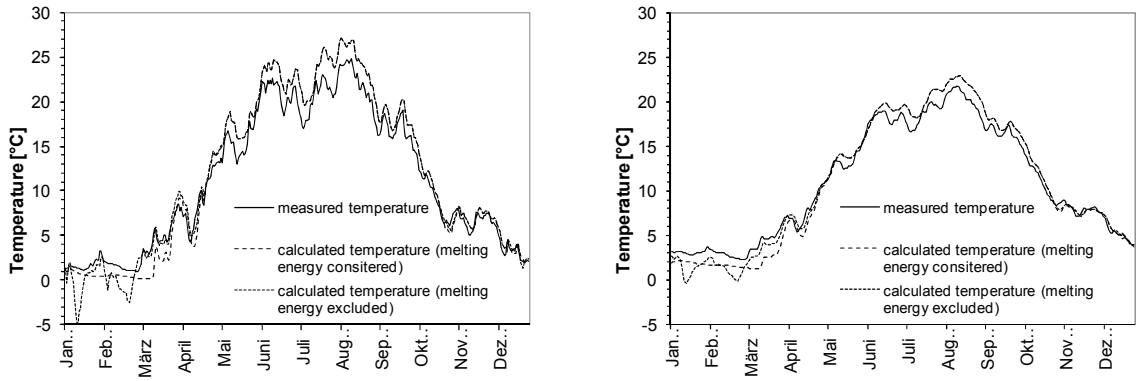

Figure 4 - Exemplary comparison of measured and numerical simulated temperatures in soils in depth of 50 cm (left) and 100 cm (right); station dresden, year

2.3 Frost in pavement structures - damages

Frost in pavement sub layers and the associated damage process are well known. In addition to lifting effects (formation of ice lenses) as a result of volume increasing during the freezing process, the temporary reduce of load capacity is a result of insufficient or interrupt drainage ability of soils. Thus melting water can't sweep away because deeper layers are still frozen (Figure 6 – left). Of Course the presence of water is necessary for these problems.

The definition of the frost proof pavement thickness is regulated by the guidelines for the standardization of road constructions RStO [6] or by the guidelines for the asphalt design process RDO Asphalt [7] in the same way. To avoid damages as a result of frost penetration in pavement structures, a thickness of 60 % of the maximum frost penetration ($z_{F\ max}$) is enough according to the existing experience [17]. In the current version of the guidelines the definition of the frost proof pavement thickness based on the frost penetration of the winter 1962/1963, the so called dimensioning winter. Recent studies of the Germany's National Meteorological Service (DWD) have shown that such a winter has a return period of more than 100 years [19]. Based on the weather data recording of the DWD (10 weather stations) over the years 1991 till 2004, the temperatures in pavements (reference pavement structure to Figure 1) are simulated continuously for different German regions. Figure 5 shows on the left side exemplary for a pavement system according to RStO (construction class III) [6] and defined material specific parameters the calculated frequency of exceedance.

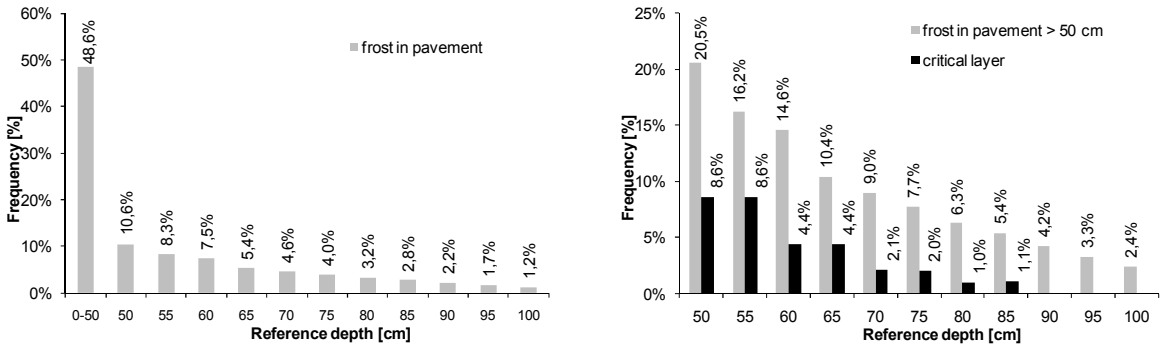

Figure 5 - Frequency of exceedances of frost in pavement structures (left); Frequency of exceedances of frost deeper than > 50 cm (normalized to 100 %) and the part of exceedances of critical layers (right)

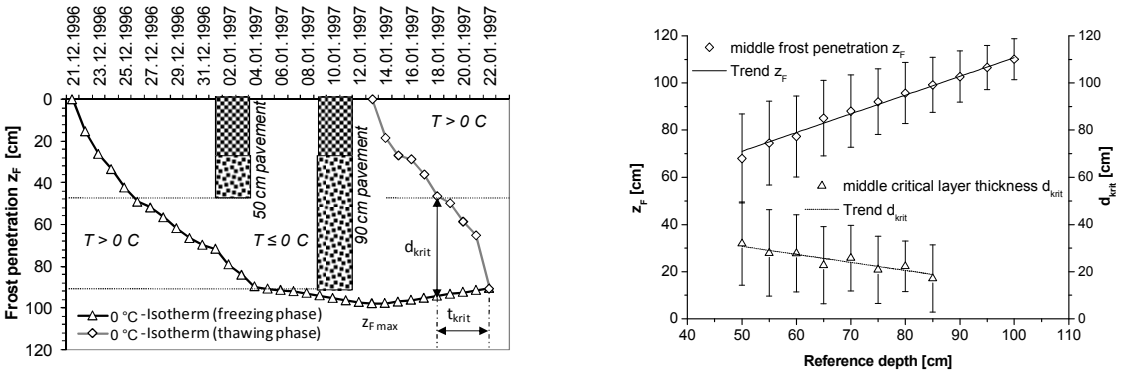

Figure 6 - Qualitative freezing-thawing process presentation of the maximum frost depth ($z_{F\ max}$) and the critical layer thickness (d_{krit}) according the reference depth (left); average frost penetration and average of critical layer thickness according the reference depth (right)

About the half (48, 6 %) of all frost penetrations don't reach depths over 50 cm and therefore no sub ground. The right side of Figure 5 shows the distribution of frost penetrations with depths greater than 50 cm (normalized to 100 %) and the part of exceedances of critical layers and thus reduced bearing capacity. As could be expected, the exceedances of frost is reduced with increasing reference depth. Depths greater than 50 cm and therefore important for the dimensioning process are reached by 50 % of all frost events. Critical layers appears comparatively rare but with thicknesses of up to 30 cm. Generally it is important for a dimensioning design process to know changes of the mechanical behavior of soil and grain during frost or insufficient or interrupt drainage ability. This very complex material performance is not the subject of this study and part of other research projects. Against the background of the projected climate change it is very interesting for future pavement designs, which trends of change (frost penetration depth and critical layers) are expected. Following, the emission scenarios for the numerical simulation will be presented and also the results of the calculation for a selected area.

2.4 Emission scenario

Numerous measurements and observations of different institutions show a clear increase of the greenhouse gas concentration since the 1950s. The enormous influence of these at the energy balance of our climate system leads to a positive ray forcing and thus to a heating of the air layers close to the surface [2]. Since the beginning of the measurement with instruments in 1850 the middle global temperatures of the air layers close to the surface increases continuously. In the 20th century the middle increase was approximately 0,6 K ± 0,2 K [1]. In the last few years this temperature increase resulting from the climate change was palpable. 11 years in the period of 1995 to 2006 belongs to 12 warmest years since 1950 [2].

The effects of climate change are regionally very different. While the middle of the global air temperature close to the surface increased approximately 0,6 K [1] during the 20th century, the increase in Europe records even 0,8 K [8]. The analysis of the climate development for Germany shows a increase of 0,9 K [9; 10] in the equal time period. To forecast the future development of our climate system different emission scenarios (Special Report on Emissions Scenarios - SRES) are shown in [1; 2]. The base of this emission scenarios are the projected developments of the world economy. These scenarios ranges from an acceptance of a fast grow of the world economy with intensive use of fossil fuels to a acceptance of using clean and resource-saving technologies by decreasing consumption of materials. Excluded from these scenarios are influences, resulted on the realization of the United Nations Framework Convention (United Nations

Framework Convention on Climate Change – UNFCCC) or the Kyoto protocol. Model calculations to forecast the future climate change show, that the heating of our climate increases approximately 0,1 K per decade without a increasing concentration of greenhouse gas and therefore by constant ray forcing based on the year 2000. If the concentration of the greenhouse is not constant but increasing, the average heating will be approximately 0,2 K to approximately 0,4 K per decade [1].
For thermal simulations were used projected and provided climate data of the group models and data (M&D) from the Max Planck Institute for Meteorology Hamburg. Base of it was the IPCC- emission scenario A1B [11]. The scenario assumes a fast growing of the word economy by a balanced using of all energy sources. The model calculation realized at the Max Planck Institute for Meteorology Hamburg (emission scenario A1B) is performed in two calculation runs with different starting conditions.
Based on the projected changes of the environmental conditions, the temperatures of the pavement surface of both model calculations of scenario A1B were numerical simulated. This simulation was realized for a pavement structure according to Figure 4 for the area of Dresden City and surrounding (Longitude; 13,6° - 13,8°; Latitude: 51,0° - 51,2°) over a period from 2001 to 2069. The selected area includes 4 grid points and an area of 318, 9 km².
The shown results of the thermal simulations base on the average data of the decisive climate parameters of the used 4 gird points and therefore the results are averages of the defined area. To compare and to assess the results of the modeling scenarios A1B, that means the change of the thermal condition in pavements, the climate simulation C20 (Climate of the 20th Century) over a period from 1980 to 2000 was used [12].

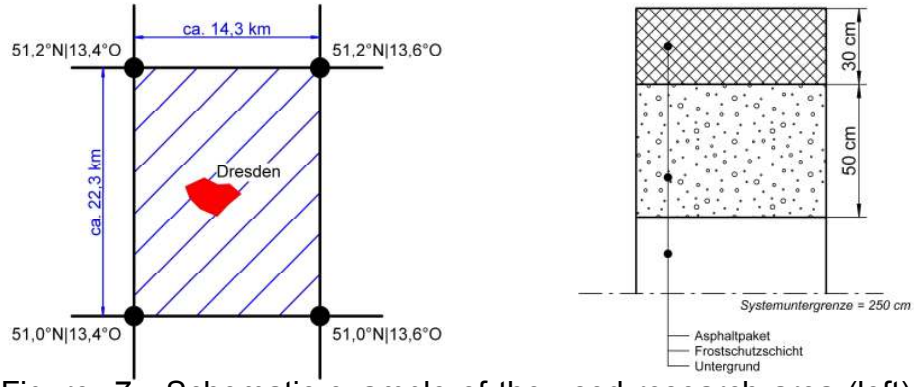

Figure 7 - Schematic example of the used research area (left) and the used pavement structure (right)

3. FORECAST OF TEMPERATURE CONDITIONS IN PAVEMENT

3.1 Conventions of temperature simulation - parameter definitions

The following material conventions for the numerical simulations were determined:

Reflective properties of asphalt:
- Reflectivity for short wavelength radiation α_k = 0,15
- Reflectivity for long wavelength radiation α_l = 0,05
- Thermal conductivity λ = 1,05 W/m²
- Specific heat capacity c_p=878 W·s/(kg·K)
- Density ρ = 2240 kg/m³

Properties of sub base (UGM):
- Thermal conductivity (for T > 0°C) λ = 2,14 W/m²
- Thermal conductivity (for T ≤ 0°C) λ = 1,70 W/m²

- Specific heat capacity (for c_p > 0°C) c_p =837 W·s/(kg·K)
- Specific heat capacity (for c_p ≤ 0°C) c_p =767 W·s/(kg·K)
- Density ρ = 2050 kg/m³
- Gravimetric water contend w_g = 3,5 M.-%
- Approximation coefficient (temperature dependent unfrozen water part) Z = 5

Properties of sub ground:
- Thermal conductivity (for T > 0) λ = 1,60 W/m²
- Thermal conductivity (for T ≤ 0) λ = 1,82 W/m²
- Specific heat capacity (for c_p > 0°C) c_p =1173 W·s/(kg·K)
- Specific heat capacity (for c_p ≤ 0°C) c_p =900 W·s/(kg·K)
- Density ρ = 1780 kg/m³
- Gravimetric water contend w_g = 15 M.-%
- Approximation coefficient (temperature dependent unfrozen water part) Z = 1,5

3.2 Temperatures on the pavement surface

The results of the temperature simulation show that based on the mentioned conditions according to, emission scenario A1B and the determined thermal material parameters it is probable to expect a considerable change of the pavement surface temperature and therefore thermal pavement condition.
Related to a period of 30 years starting in 1980 to 2009 it is expected that the 30-year average of the pavement surface temperatures increase by the end of the first half of the 20th century approximately 0,8 K to 0,9 K. By the end of the simulation period the increase reaches approximately 1,6 K to 1,8 K (Figure 8 – left). The changes of the average of the 30-year minimum of the pavement surface temperatures are more impressive. Already in the next 30 years the increase is projected by approximately 1,3 K to 1,7 K (Figure 8 – right). To the end of the simulation period 4,8 K to 5,0 K will be reached. The plausibility is provided by direct correlation of the simulated temperatures of pavement surface and the air temperatures projected by the Max Planck Institute for Meteorology (Figure 9).

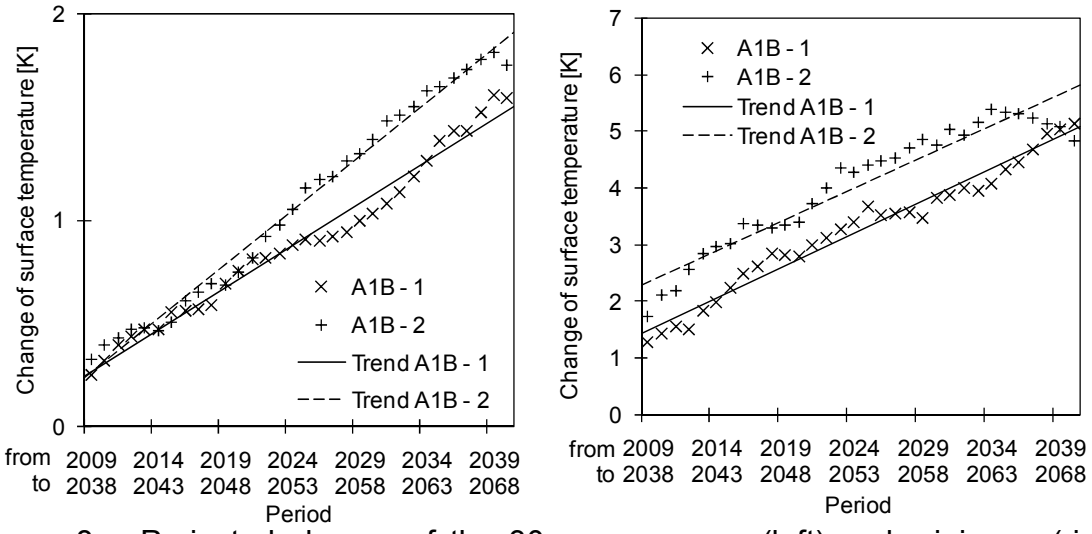

Figure 8 – Projected change of the 30-year average (left) and minimum (right) of the pavements surface temperatures – period: 1980 to 2009

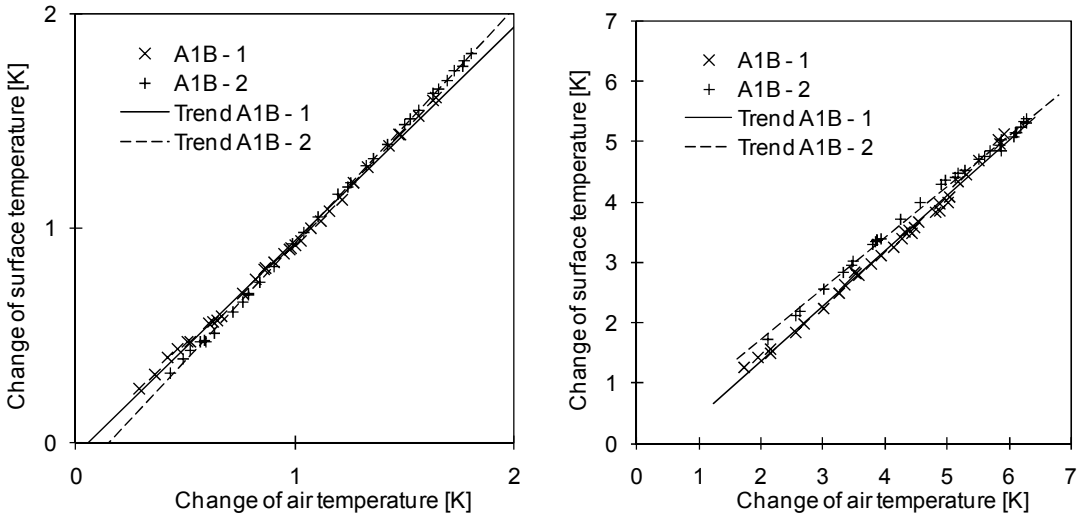

Figure 9 – Compare of projected change of the 30-year average (left) and minimum (right) of the air- and surface pavement temperature (period 1980 to 2009)

Generally it is possible, that the frequency of negative pavement surface temperatures will be decreasing in the next years (Figure 10 – right). However there will be single years with cold temperatures compared to the 30-year average and therefore show a high part of negative pavement surface temperatures (Figure 10 – left). For the temperature conditions in pavements are expected similar developments, because the temperatures in pavements are strictly coupled with the pavement surface temperature.

The frost penetration in pavements depends on intensity and duration of negative pavement surface temperatures and also of thermo-physical material parameters of each single layer. If one looks at the frequency of the negative average daily temperature in depths of 50 and 90 cm under pavement surface, one can see a reduction by about 50 % (Figure 11).

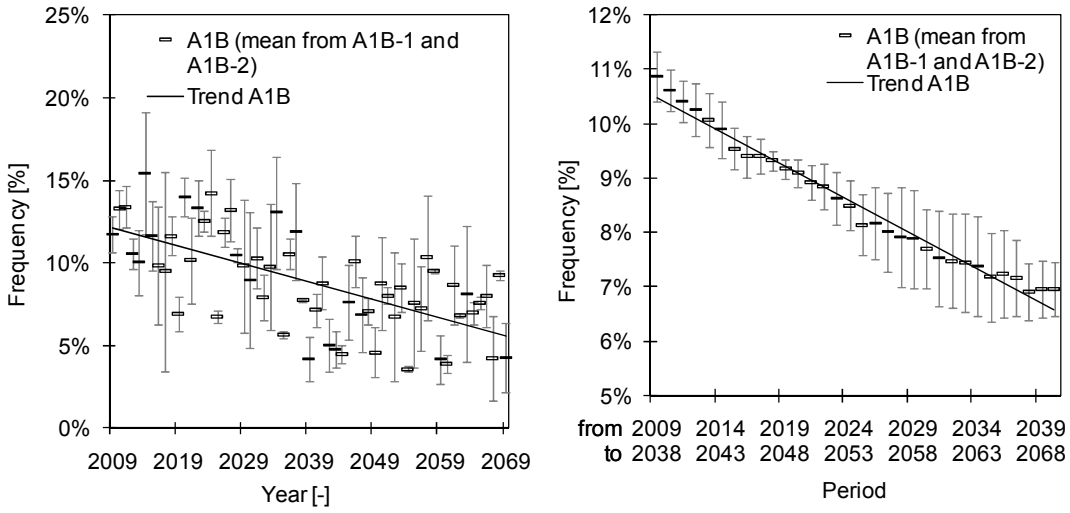

Figure 10 – Projected frequency of negative pavement surface temperatures (left); 30-year average (right); the error index describes the range of the two scenario runs

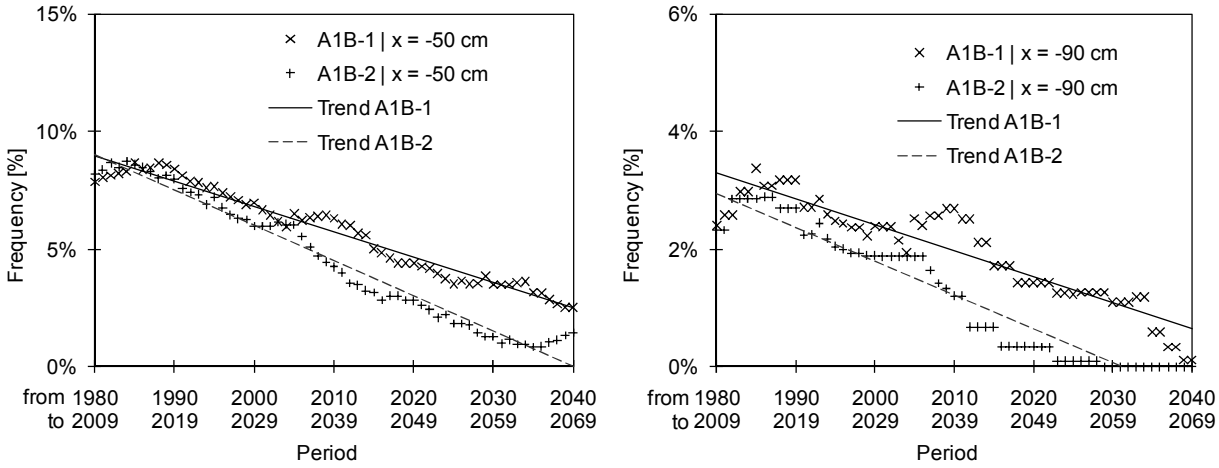

Figure 11 – Frequency of negative average daily temperatures in depths of 50 and 90 cm under pavement surface

4. DIMENSIONING THE FROST PROOF THICKNESS

As part of an economical dimensioning of the frost proof thickness, there are efforts to use a dimensioning winter or dimensioning frost penetration based on a 30-year recurrence interval.

$$\Psi = \frac{1}{1 - f(z_F)} \qquad \text{(II)}$$

with:

ψ	recurrence interval [years]
z_F	yearly frost penetration [cm]
$f(z_F)$	distribution function [-]

The calculated yearly frost penetration, based on the thermo-physical simulation, can be good represented by using a normal distribution (Figure 12 – left). Based on equation II, the frost penetration for any recurrence interval is determinable using the needed parameters expectation and standard deviation. For a period of 1980 to 2009, the maximum frost penetration for the 30-year recurrence interval was approximately 115 cm. Therefore the necessary thickness of the frost proof pavement structure is 70 cm in accordance to the mentioned German guidelines. Figure 12 – right shows the changes of the maximum frost penetration which are necessary for the dimensioning process (30-year recurrence interval) depending on the projected period.

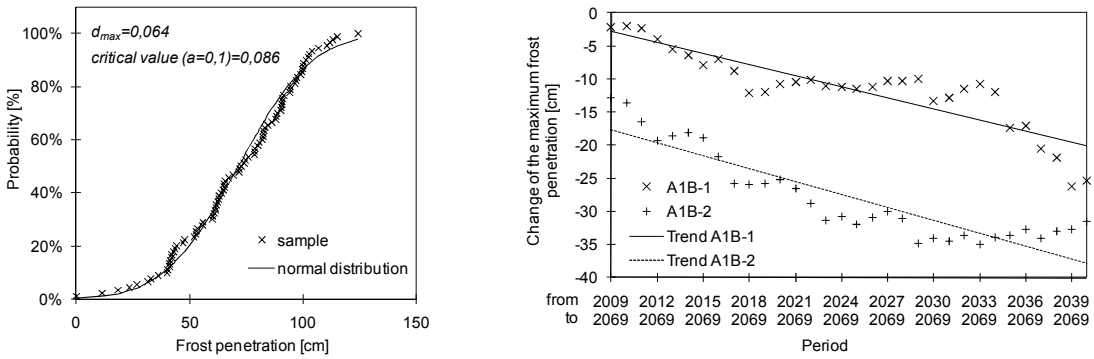

Figure 12 – Adaption of the yearly maximum of frost penetration to an normal distribution (left); Projected change of the maximum frost penetration necessary for the dimensioning process based on a 30-year recurrence interval (right)

$$\Delta z_{F,30}^{t\to 2069} = z_{F,30}^{t\to 2069} - z_{F,30}^{1980\to t} \quad \text{(III)}$$

mit:

$\Delta z_{F,30}^{t\to 2069}$ Differences of thickness of frost penetration for a period of t to 2069 based on a 30 year recurrence interval [cm]

$z_{F,30}^{t\to 2069}$ frost penetration for a period of t to 2069 based on a 30 year recurrence interval [cm]

$z_{F,30}^{1980\to t}$ frost penetration for a period of 1980 to t based on a 30 year recurrence interval [cm]

The differences of thickness calculated with equation III are referred to the maximum frost penetration of the last period, starting in 1980 to the beginning of the projected period. The sample size minimum was determined with n=30 (30 years) and therefore the distribution parameters are defined adequately. Already in the second third of this century the maximum of the expected frost penetration will be about 10 to 30 cm lower. This result shows clearly, that the necessary thickness of the pavement structure can be reduced in future between 6 and 12 cm. Figure 12 presents the reduction of thickness. It is important, that the reduction refers only to the criterion frost proof according to the design process [6; 7]. To estimate which further effects result from a possible reduce of thickness, the necessary proofs according to the German design process [7] were done, for three asphalt pavement structures according to construction classes SV, III and V, Line 1 [6]. The used calculation based on three different thicknesses of the frost proof layer of each construction class (Table 1). Furthermore the material parameters of the defined calibrating asphalt and the axle load spectrum called “long distance traffic” for construction class SV and “suburban traffic” for construction class III and V were used [7]. The used number of axle load cycles of the three construction classes was defined in that way, that the version with the greatest thickness of the frost proof layer (version 3) fulfilled the three necessary proofs:

1. Plastic deformation of sub ground
2. Plastic deformation of UGM
3. Fatigue proof of asphalt base layer

Reference period for temperature conditions was 1980 to 2009.

For construction class SV and III, the fatigue proof of asphalt base layer was decisive for determining the existing number of axle load cycle. For construction class V on the other hand the proof of the plastic deformation of UGM was decisive. The following numbers of axle load cycles are defined.

- Construction class SV → N_{vorh} = 38.800.000
- Construction class III → N_{vorh} = 2.620.000
- Construction class V → N_{vorh} = 196.000

Table 1 – Material parameter; *) clip values present the thickness of the asphalt layers (surface-, binding- and base corse) [cm]

Construction class SV (4|8|22)*)	VAR1	VAR2	VAR3
Pavement thickness [cm]	65	75	85
Thickness of sub base [cm]	31	41	51
E_{v2} on surface of sub base [N/mm²]	120	120	120
Elastic modulus of sub base [N/mm²]	186	164	141
E_{v2} on formation [N/mm²]		45	
Construction class III (4|4|14)*)	VAR1	VAR2	VAR3
Pavement thickness [cm]	55	65	75
Thickness of sub base [cm]	33	43	53

E_{v2} on surface of sub base [N/mm²]	120	120	120
Elastic modulus of sub base [N/mm²]	182	159	136
E_{v2} on formation [N/mm²]		45	
Construction class V (4|10)[*)]	VAR1	VAR2	VAR3
Pavement thickness [cm]	45	55	65
Thickness of sub base [cm]	31	41	51
E_{v2} on surface of sub base [N/mm²]	120	120	120
Elastic modulus of sub base [N/mm²]	186	164	141
E_{v2} on formation [N/mm²]		45	

Figure 13 shows the total deformation based on the MINER – hypothesis (MINER-Total) for the three proofs considering the changed thicknesses of sub base and the construction classes and period. The results show that by using the determined conditions, a reduction of the sub base thickness for reason of lower frost risk for construction class V is not possible. Already a minor decrease of the sub base thickness results in plastic deformations with destructive characteristic. Different are the effects in the construction classes SV and III. The MINER-Total of the fatigue proof increases continuously with a sub base becoming even smaller. A new balance can be reach by a slightly larger thickness of the asphalt base. The proof of plastic deformation of UGM will be decisive for both construction classes by reducing the sub base of more than 18 cm.
The forecast calculations show, that even under, the changing climate conditions of the presented period from 2009 to 2069, a reduction of the sub base thickness of 10 cm (construction class SV and III) will cause no plastic deformations of sub ground in a damaging (Figure 14 - below). By a reduction of 15 cm damages can be expected for construction class SV starting in the second half of the century. Plastic deformations of UGM in a damaging way are not expected for the projected period (Figure 14 – middle). Obviously, the trend of the MINER-Totals will also increase for this proof especially for the second third of this century.
Essentially serious are the effects of the future climate change according to the fatigue proof. The MINER-Total will exceed the values from the period 1980-2009 by 20% in the next 30 years (Figure 14 – above). That increase of the MINER-Total will probably go on in future. In the second half of the century an increase of even 100 % according to the reference period is reached.

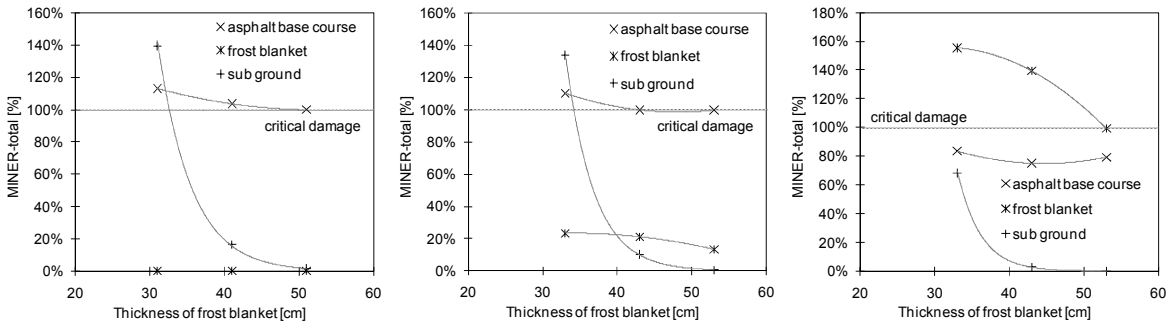

Figure 13 - MINER-Total of the three proofs according to RDO-A [7] by variation of the UGM thickness for construction class SV (left), III (middle) and V (right)

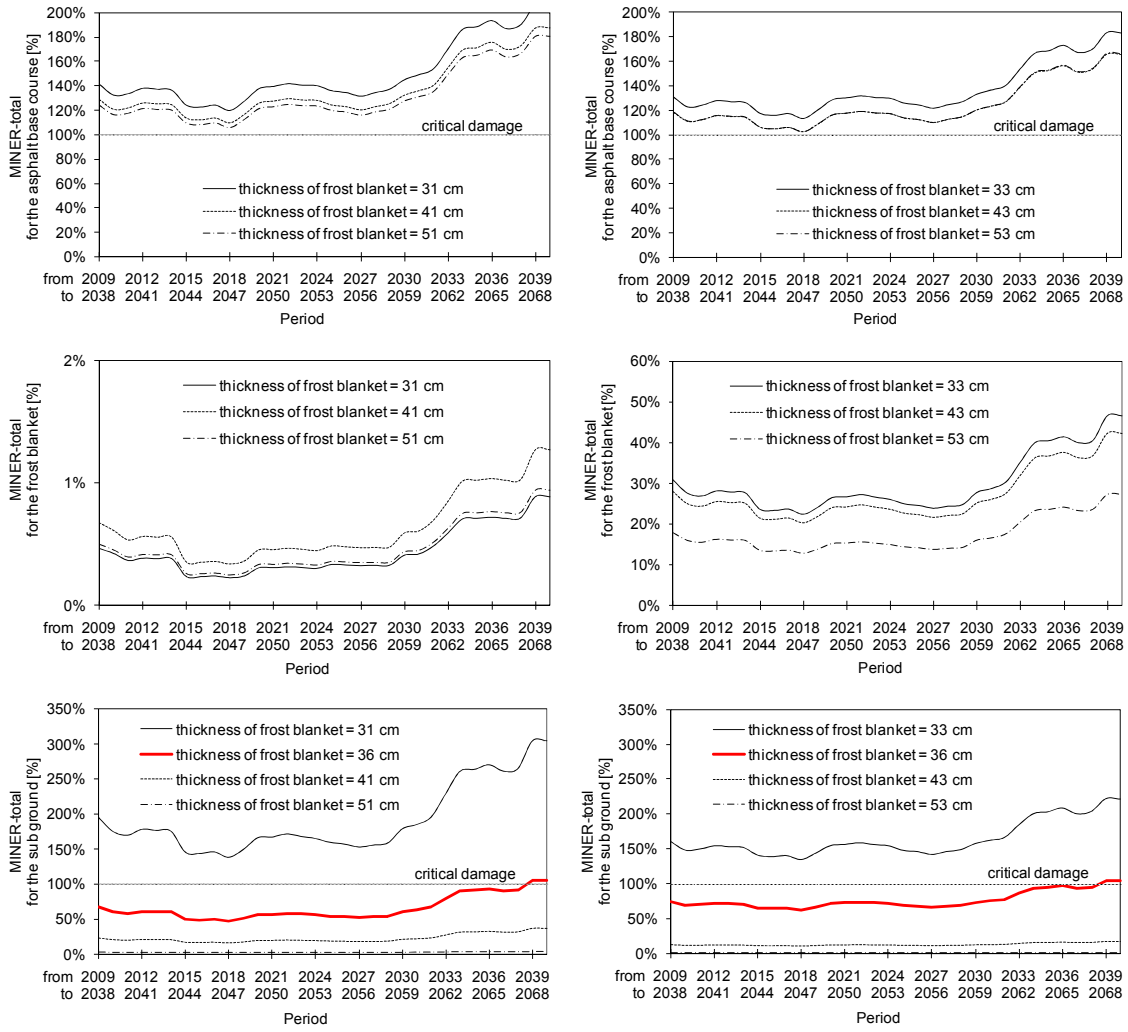

Figure 14: Projekted MINER-Total of the three proofs according to RDO-A [7] by variation of the UGM thickness for construction class SV (left) and III (right)

5. SUMMARY

As part of this investigation was shown, that the projected climate change according to the IPCC-Scenarios A1B [11] have effects on the temperature conditions in pavements. The results of the thermal simulations based on the climate scenarios show, that the minimum of the temperatures, the negative temperatures in generally and their frequency are decreasing. Based on these results was shown, that the maximum of frost penetration will be reduced. The logical consequence from an economic view is a reduction of pavement thickness. Using the German design process [7] three construction classes (SV, III and V) were analyzed. Aim was to investigate the expected effects concerning to the pavement stability resulting from a possible reduction of the sub base thickness.

It can be observed, that even by highly stressed pavements with a comparatively great thickness of the bounded layers, a reduction of the thickness of UGM is possible without a significantly larger damage risk of the unbound layer. Irreversible deformation in a destructive dimension can be expected for the secondary road network, with a comparatively small thickness of the bounded layers. Essentially more drastic are the effects of the projected climate change referring to the fatigue of the asphalt base layer. Even without a reduction of the sub base thickness, the fatigue of the asphalt base layer will be increase more quickly by considering the IPCC-Scenarios A1B.

It should be noted, that the calculation based on linear elastic material behavior for the whole pavement and also for the sub ground. Therefore the presented results have to be verifyed with calculations based on non linear material behavior.

LITERATURE

1. IPCC (2001). Zusammenfassung für politische Entscheidungsträger. In: Klimaänderung 2001. Dritter Sachstandsbericht des Zwischenstaatlichen Ausschusses für Klimaänderung (IPCC). Deutsche Übersetzung durch ProClim-, Bern, 2002
2. IPCC (2007). Zusammenfassung für politische Entscheidungsträger. In: Klimaänderung 2007. Vierter Sachstandsbericht des Zwischenstaatlichen Ausschusses für Klimaänderung (IPCC). Deutsche Übersetzung durch ProClim-, österreichisches Umweltbundesamt, deutsche IPCC-Koordinationsstelle, Bern/Wien/Berlin, 2007
3. Brehm, D.R. (1989). Entwicklung, Validierung und Anwendung eines dreidimensionalen, strömungsgekoppelten finite Differenzen Wärmetransportmodells. Justus-Liebig-Universität Giessen, Fachbereich Geowissenschaften und Geographie
4. Lottmann, A. (2003). Tragfähigkeit und Frostempfindlichkeit von kalkbehandelten bindigen Böden im Planumsbereich von Verkehrsflächen. Dissertation, Brandenburgische Technische Universität Cottbus, Fakultät Architektur, Bauingenieurwesen und Stadtplanung
5. Unold, F. (2006). Der Gefriersog bei der Bodenfrostung und das Kompressionsverhalten des wieder aufgetauten Bodens. Dissertation, Universität der Bundeswehr München, Fakultät für Bauingenieur- und Vermessungswesen
6. RSTO (2001). Richtlinien für die Standardisierung des Oberbaues von Verkehrsflächen. Forschungsgesellschaft für Straßen- und Verkehrswesen, FGSV Verlag, Köln
7. RDO Asphalt (2009). Richtlinien für die rechnerische Dimensionierung des Oberbaus von Verkehrsflächen mit Asphaltdecke. Forschungsgesellschaft für Straßen- und Verkehrswesen, FGSV Verlag, Köln
8. Leuschner, Ch.; Schipka, F. (2004). Klimawandel und Naturschutz in Deutschland. Abschlussbericht eines F+E-Projekt (FKZ: 80383010), BfN-Skripten 115, Bundesamt für Naturschutz, Bonn
9. Hulme, M.; Sherd, N. (1999). Climate Change Szenarios for Germany. Climate Research Unit. Norwich, UK, 6pp
10. Schönwiese, C.-D., et al. (2003). Klimastatement 2003. Deutsche Meteorologische Gesellschaft, Österreichische Gesellschaft für Meteorologie, Schweizer Gesellschaft für Meteorologie, Aktualisierte Fassung vom September 2003
11. Lautenschlager, M.; Keuler, K.; Wunram, C.; Keup-Thiel, E.; Schubert, M.; Will, A.; Rockel, B.; Boehm, U. (2006). Climate Simulation with CLM, Scenario A1B run no.1 and run no. 2, Data Stream 3: European region MPI-M/MaD. World Data Center for Climate
12. Lautenschlager, M.; Keuler, K.; Wunram, C.; Keup-Thiel, E.; Schubert, M.; Will, A.; Rockel, B.; Boehm, U. (2008). Climate Simulation with CLM, Climate of the 20th Century run no.1, Data Stream 3: Euro-pean region MPI-M/MaD. World Data Center for Climate
13. Kayser, S.; Wellner, F. (2008). Grundlagen zur Erfassung der Temperaturbedingungen für eine analytische Bemessung von Asphaltbefestigungen. Forschung Straßenbau und Straßenverkehrstechnik, Heft 996, Bundesministerium für Verkehr, Bau und Stadtentwicklung, Bonn
14. Patzak, J.; Kayser, S; Wellner, F. (2010). Überprüfung und Bewertung der Frostdimensionierung nach den RStO.Forschung Straßenbau und Straßenverkehrstechnik, Heft 1045, Bundesministerium für Verkehr, Bau und Stadtentwicklung, Bonn
15. Smoltczyk, U. (2001). Grundbau-Taschenbuch 2. Geotechnische Verfahren, 6. Auflage, Ernst W. + Sohn Verlag, Berlin
16. Williams, W. M.; Schild, K.; Dinter, S.; Stricker, D. (2007). Bauphysik, Formeln und Tabellen. Vieweg+Teubner Verlag, Wiesbaden, 2007
17. FGSV (1994). Entstehung und Verhütung von Frostschäden an Straßen. Arbeitsausschuss Frost. Schriftenreihe der Forschungsgesellschaft für Straßen- und Verkehrswesen 105. Bundesministerium für Verkehr, Bau und Stadtentwicklung, Kirchbaum Verlag, Bonn
18. Farouki, O. T. (1986). Thermal Properties of Soils. Series of Soil Mechanics Vol. 11
19. Gerth, W.-P.; Roose, M.; Augter, G. (2008). Aktualisierung der Frostdimensionierung im Straßenbau. Forschung Straßenbau und Straßenverkehrstechnik, Heft 1002, Bundesministerium für Verkehr, Bau und Stadtentwicklung, Bonn